JACS Au
AN OPEN ACCESS JOURNAL OF THE AMERICAN CHEMICAL SOCIETY

pubs.acs.org/jacsau
Article

Paralogue-Selective Degradation of the Lysine Acetyltransferase EP300

Xuemin Chen,[⊥] McKenna C. Crawford,[⊥] Ying Xiong,[⊥] Anver Basha Shaik, Kiall F. Suazo, Ludwig G. Bauer, Manini S. Penikalapati, Joycelyn H. Williams, Kilian V. M. Huber, Thorkell Andressen, Rolf E. Swenson, and Jordan L. Meier*

Cite This: JACS Au 2024, 4, 3094−3103

ABSTRACT: The transcriptional coactivators EP300 and CREBBP are critical regulators of gene expression that share high sequence identity but exhibit nonredundant functions in basal and pathological contexts. Here, we report the development of a bifunctional small molecule, MC-1, capable of selectively degrading EP300 over CREBBP. Using a potent aminopyridine-based inhibitor of the EP300/CREBBP catalytic domain in combination with a VHL ligand, we demonstrate that MC-1 preferentially degrades EP300 in a proteasome-dependent manner. Mechanistic studies reveal that selective degradation cannot be predicted solely by target engagement or ternary complex formation, suggesting additional factors govern paralogue-specific degradation. MC-1 inhibits cell proliferation in a subset of cancer cell lines and provides a new tool to investigate the noncatalytic functions of EP300 and CREBBP. Our findings expand the repertoire of EP300/CREBBP-targeting chemical probes and offer insights into the determinants of selective degradation of highly homologous proteins.

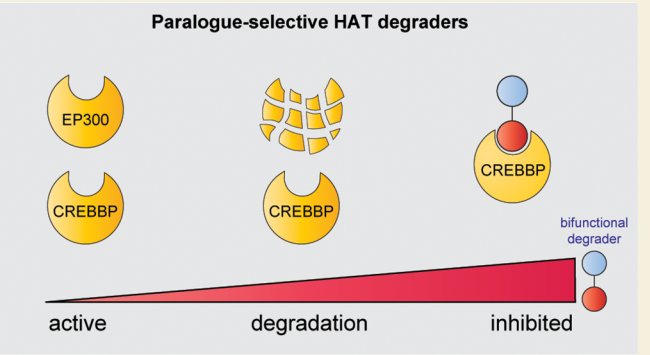

KEYWORDS: *EP300, acetyltransferase, epigenetics, inhibitors, degradation*

The paralogous transcriptional coactivators EP300 and CREBBP are critical regulators of transcription signaling in biology and disease.[1] Within the nucleus, these high molecular weight (~300 kDa) enzymes engage partner proteins through an array of protein−protein interaction motifs. Many of these proteins, including histones and transcription factors, serve as substrates for the catalytic histone acetyltransferase (HAT) domain embedded in the core of these proteins (Figure 1). As central nodes in transcriptional signaling, EP300 and CREBBP have been implicated in both oncogenic and tumor suppressive function in cancer.[2] However, despite their strong similarity, EP300 and CREBBP do not appear to be functionally redundant across all biological contexts. For instance, genetic disruption of EP300 alone is sufficient to impair the leukemogenicity of the AML1-ETO transcription factor[3] and facilitate antitumor autoimmunity in T-regulatory cells.[4] Conversely, CREBBP alone constitutes a unique nononcogene dependency in EP300-deficient cancers[5] and is required for hematopoietic stem cell self-renewal in mice.[6] To date, paralogue-specific functions of EP300 and CREBBP have been almost exclusively studied using genetic methods.

From a small molecule perspective, significant efforts have led to the development of potent and selective inhibitors of the EP300 and CREBBP HAT domains.[7,8] One of the most potent of these compounds is CPI-1612.[9,10] In biochemical assays CPI-1612 disrupts EP300 and CREBBP catalytic activity at half-maximal inhibitor concentrations of <0.5 and 2.9 nM, respectively (Table S1). Considering how this narrow selectivity window may be leveraged to study individual functions of EP300 and CREBBP, we were inspired by recent examples from the targeted protein degradation literature.[11] This strategy entails the construction of bifunctional molecules that induce proximity between a target protein and an E3 ligase, which in turn triggers the target's ubiquitinylation and proteasomal degradation. In one example, conversion of a dual CDK4/CDK6 ligand into a bifunctional enabled selective degradation of CDK6.[12] Most EP300/CREBBP degraders reported to date engage the bromodomain and cause dual degradation of both paralogues.[13−16] One degrader based on the HAT inhibitor A-485 has been shown to selectively degrade EP300 in neuroblastoma models.[17] However, we found this molecule does not have significant activity in HAP-1

Received: May 16, 2024
Revised: July 5, 2024
Accepted: July 5, 2024
Published: July 29, 2024

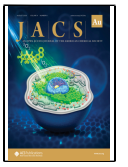

https://doi.org/10.1021/jacsau.4c00442
JACS Au 2024, 4, 3094−3103

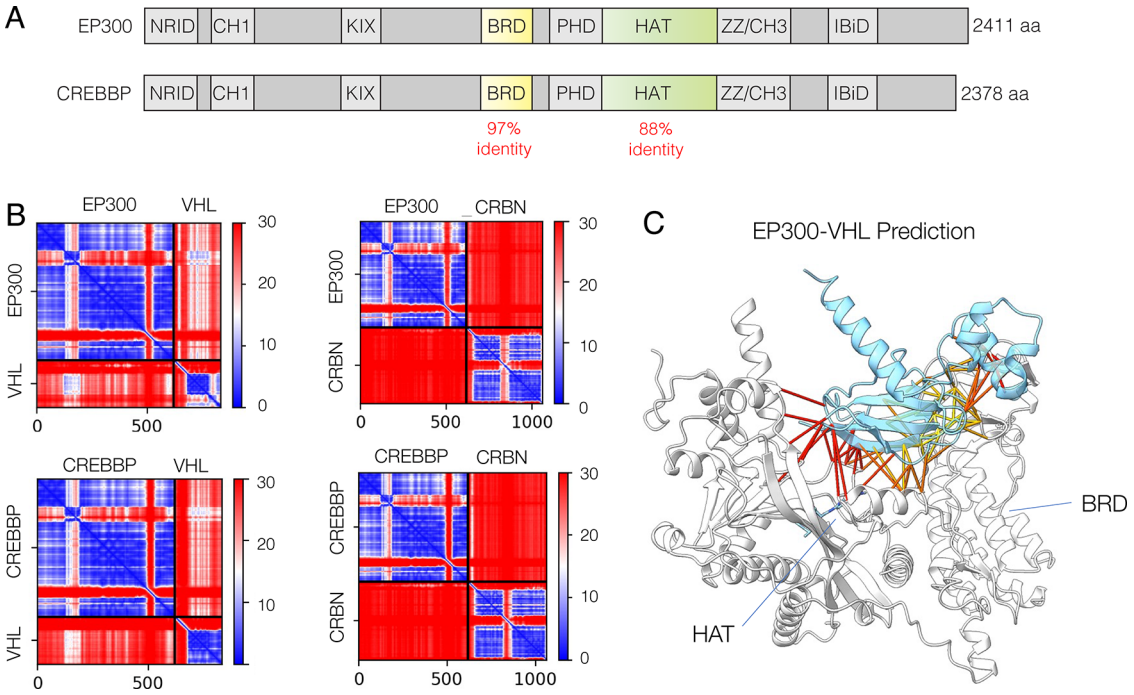

Figure 1. (A) Domain architecture of EP300 and CREBBP. The relative percent identity of two domains targeted by small molecules is specified. BRD = bromodomain, HAT = histone acetyltransferase domain. (B) AF-Multimer-generated 2D plot of predicted alignment error from predictions of EP300-E3 ligase and CREBBP-E3 ligase complexes. CRBN = cereblon, VHL = von Hippel-Lindau disease tumor suppressor. Predicted interactions are found in the top right and bottom left panels, where blue corresponds to lower estimated error. (C) AF-Multimer predicted structure of EP300 catalytic core (white) bound to VHL (blue). The majority of predicted interactions are with residues found in the EP300 HAT domain. All predictions were made using Colabfold.[19]

Scheme 1. Synthesis of CPI-1612-Based Degrader Molecules[a]

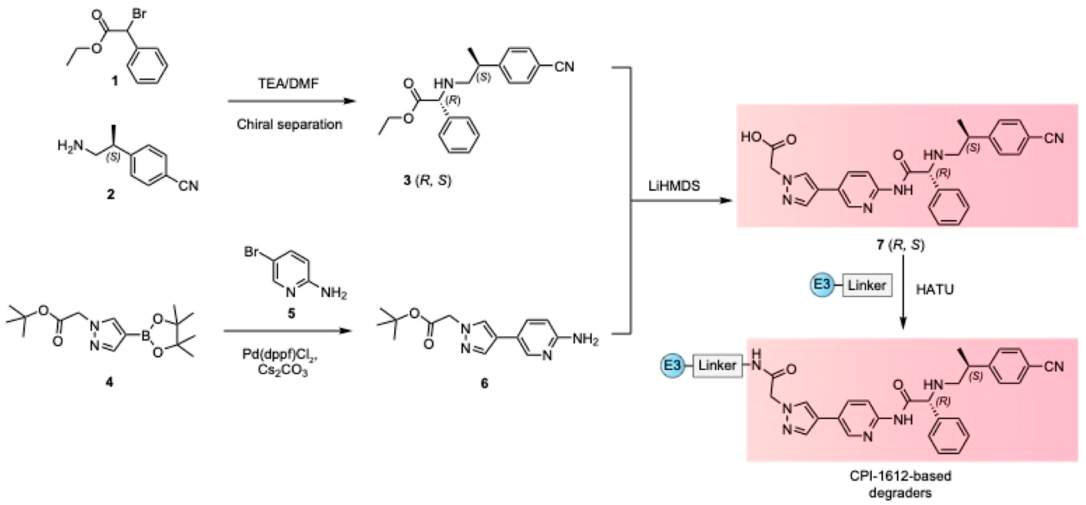

[a]Full synthetic details are provided in the Supporting Information.

cells (Figure S1), suggesting further exploration of paralogue-specific degradation strategies could be warranted.

To explore potential avenues for differentiating these closely related proteins, we began by examining the sequence conservation between the ligandable active sites of EP300 and CREBBP. EP300 and CREBBP's HAT domains are 88% identical and 93% homologous, while their bromodomains share 97% identity and 99% homology (Figure 1a). Superimposing the nonconserved residues in the HAT domain onto a crystal structure revealed the majority lie outside the small molecule binding site (Figure S2). To assess the potential for bifunctional small molecules differentiate the two proteins based on these small changes, we used the Colabfold implementation of AlphaFold Multimer[18,19] to predict the structure of EP300 and CREBBP in complex with the most commonly recruited E3 ligases, VHL and CRBN. Different degrees of confidence were made in the predictions across the two proteins (Figure 1b). Interestingly, the majority of predicted contacts were made with the HAT region, rather than the bromodomain (Figure 1c). We take care not to overstate this observation, as recent analyses have indicated that current versions of AlphaFold are not useful for predicting

https://doi.org/10.1021/jacsau.4c00442
JACS Au 2024, 4, 3094−3103

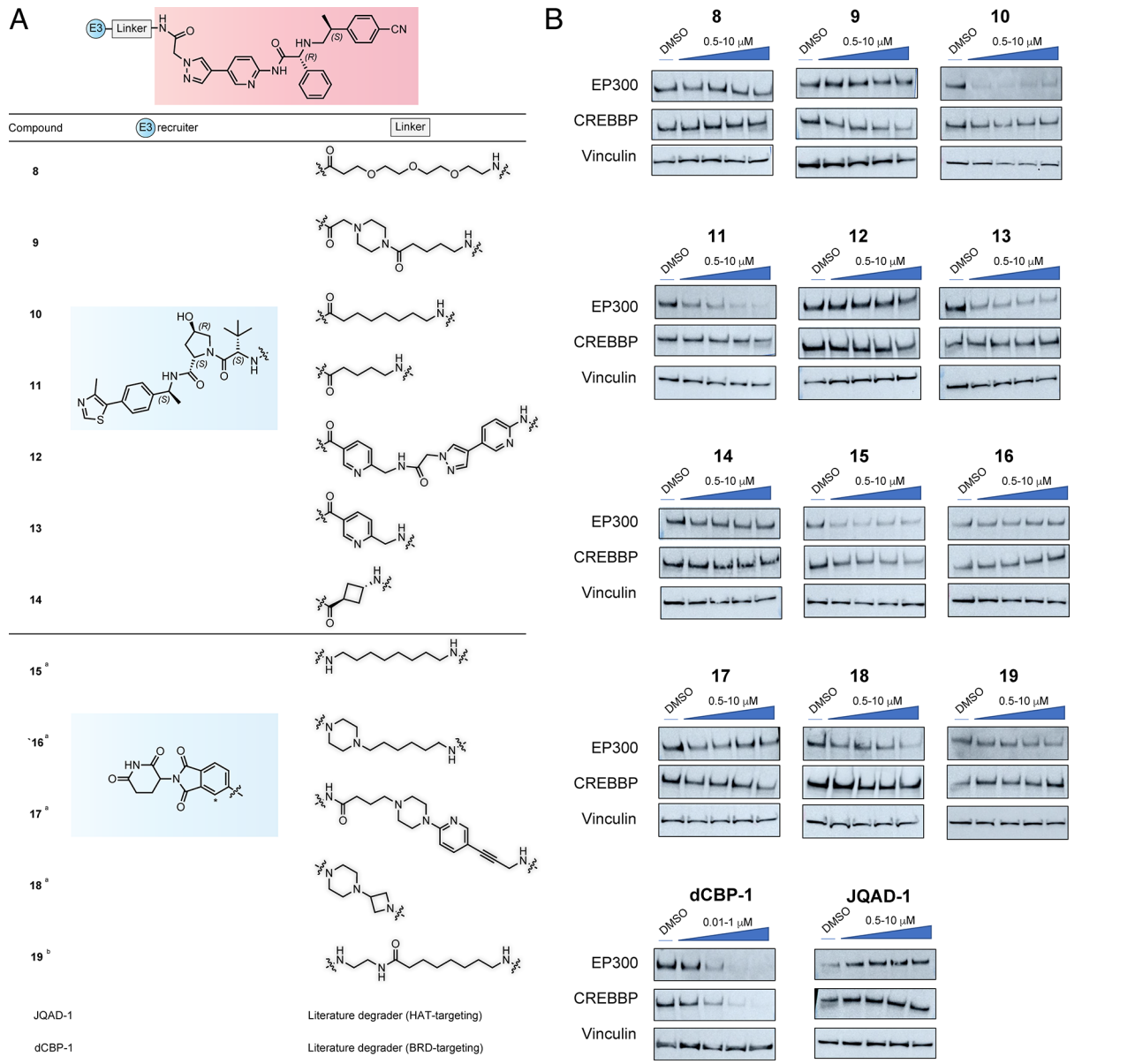

Figure 2. (A) CPI-1612-based degrader and molecules tested in this study. Compounds **8**−**14** use a VHL-recruiting ligand (blue), while compounds **15**−**19** feature a CRBN-recruiting ligand (blue). [a]Molecule tested as a mixture of diastereomers at the phenylglycine stereocenter. [b]Molecule linked CRBN ligand at the C2 position (denoted with *). Full structures are available in the Supporting Information. (B) Initial screen for modulation of EP300 and CREBBP levels at ∼24 h. Compounds **8**−**19** were tested at 0.5, 1, 5, and 10 μM. dCBP-1 was tested at 0.001, 0.01, 0.1, and 1 μM. JQAD-1 was tested at 0.1, 1, 5, and 10 μM.

the final conformation of E3 ligase/ternary complexes formed by induced proximity reagents.[20] However, the potential for differential molecular recognition, together with slight biochemical selectivity of CPI-1612 for EP300, motivated us to explore this HAT ligand's degrader capabilities.

A conjugatable analogue of CPI-1612 was synthesized via a convergent route (Scheme 1). The pyrazole amide was chosen as a suitable exit vector based on the published crystal structure of the CPI-1612/EP300 complex as well as a recent medicinal chemistry effort showing that alteration of this region is well-tolerated.[9,21] Briefly, ester **1** and amine **2** were coupled by nucleophilic displacement and purified to yield the enantiomerically pure (*R*,*S*) stereoisomer of **3**. Palladium coupling of boronate **4** with **5** provided aminopyridine **6**, which was further condensed with **3** using lithium hexamethyldisilazide to provide carboxylate **7**. Conventional amide coupling methods were then used to conjugate this precursor to a small panel of amine-containing analogues of known VHL and CRBN recruiters to afford bifunctional HAT domain ligands **8**−**19**.

As an initial test of our molecules' abilities to differentiate EP300 and CREBBP, we treated HAP-1 cells for approximately 24 h with **8**−**19** across a concentration gradient of 500−10,000 nM (Figure 2a). HAP-1 cells have previously been deployed in EP300/CREBBP degrader development.[13] Furthermore, both VHL and CRBN-recruiting bifunctionals have been shown to be active in this model.[22] Among VHL-recruiting small molecules, C8-linked compound **10** was the most potent degrader, followed by shorter C5-linked **11** and pyridine **13** (Figure 2b). All three molecules showed a preference for degradation of EP300 over CREBBP with the least potent (**13**) appearing the most selective. This contrasted with control molecule dCBP-1 which degraded both

https://doi.org/10.1021/jacsau.4c00442
JACS Au 2024, 4, 3094−3103

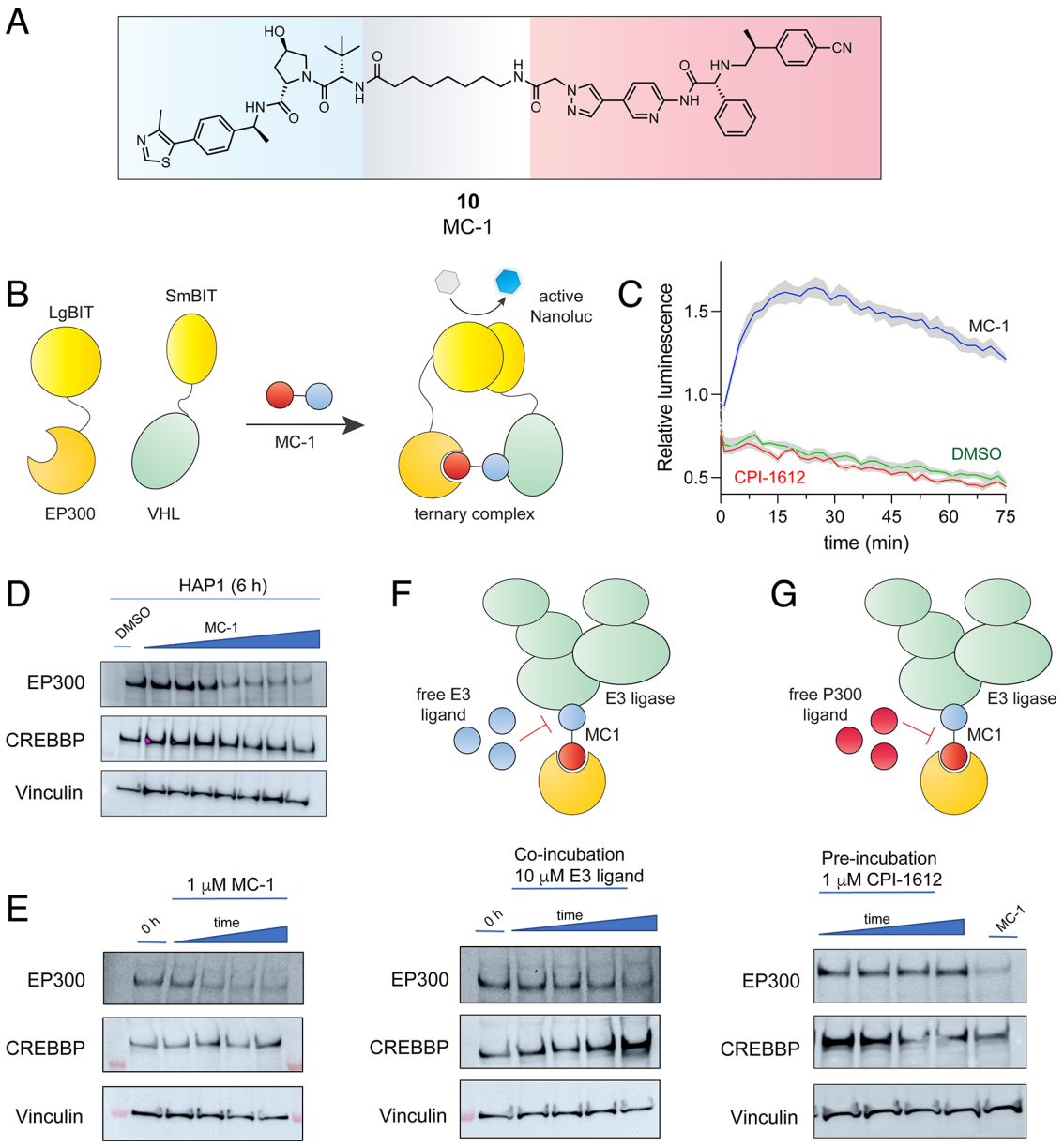

Figure 3. (A) Structure of lead degrader **10**, referred to in this manuscript as MC-1. (B) Schematic of NanoBiT assay for assessing small molecule-dependent EP300-VHL interaction. (C) Measurement of EP300-VHL binding via NanoBiT assay. Averages of 4 replicates are plotted, shaded areas represent standard deviation of mean. MC-1 and CPI-1612 were dosed at 0.25 μM. LgBIT was fused to the EP300 catalytic core (aa 1048−1664). (D) Dose-dependent degradation of EP300 at 6 h in HAP1 cells. Concentrations: 0.01, 0.05, 0.1, 0.25, 0.5, 1, 2.5 μM. (E) Time-dependent degradation of EP300 by 1 μM MC-1 in HAP1 cells. Time points: 0, 1, 3, 6, 24 h. (F) Testing the ability of free E3 ligase ligand (VH298, 10 μM) to block degradation of EP300 by MC-1 (1 μM) in HAP1 cells. Time points: 0, 1, 3, 6, 24 h. (G) Testing the ability of free HAT ligand (CPI-1612, 1 μM) to block degradation of EP300 by MC-1 (1 μM) in HAP1 cells. CPI-1612 was preincubated for 1 h before MC-1 addition. Time points (after MC-1 addition): 1, 3, 6, 24 h.

paralogues (Figure 2b).[13] Among CRBN-based degraders, **15** was the most active and also appeared to show a slight preference for EP300. However, it triggered a visibly greater maximal degradation (D_{max}) of CREBBP relative to compound **10** (Figure S3). These results suggest that recruitment of E3 ligases to the EP300/CREBBP HAT domain can trigger preferential degradation of EP300.

To qualitatively assess the ability of our ligand to directly bind endogenous full-length EP300, we synthesized an affinity probe based on the CPI-1612 scaffold and performed competitive affinity pulldown experiments using lead degrader **10** (Figure S4a), which for convenience we refer to by the abbreviation "MC-1" (Figure 3a). Our selection of **10** was due to its potent degradation of EP300 at low concentrations. In this assay, ligands are preincubated with HeLa nuclear extracts and tested for their ability to block affinity capture of EP300 or CREBBP (Figure S4b). The higher the concentration of free ligand required for competition, the weaker the binding. Compared to CPI-1612, we found that **10** only competed EP300 and CREBBP capture at higher concentrations (Figures S4c,d, S5). Cell-based assays also indicate that CPI-1612 is a more potent inhibitor of EP300/CREBBP-catalyzed acetylation than **10** (Figure S4e). Motivated by the results of our cellular experiment, we next tested whether using H3K18Ac as

https://doi.org/10.1021/jacsau.4c00442
JACS Au 2024, 4, 3094−3103

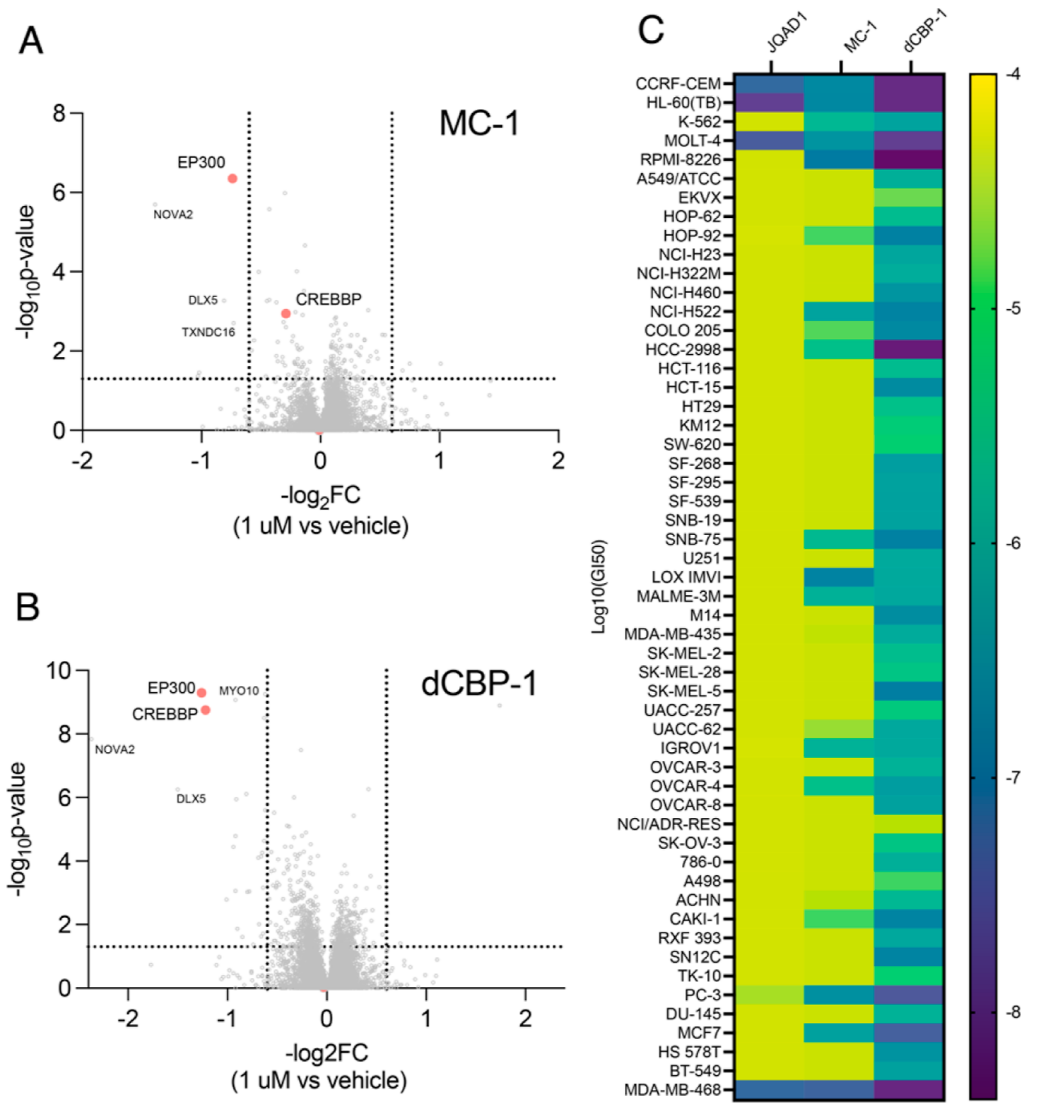

Figure 4. (A) Proteome-wide assessment of MC-1 treatment (1 μM, 6 h) in HAP1 cells with analysis of unique EP300/CREBBP peptides (n = 3 biological replicates). (B) Proteome-wide assessment of dCBP-1 treatment (1 μM, 6 h) in HAP1 cells with analysis of unique EP300/CREBBP peptides (n = 3 biological replicates). (C) Comparative analysis of half-maximal growth inhibition (GI_{50}) values for EP300 degrader molecules across the NCI-60 cell line panel (72 h incubation).

a readout for EP300/CREBBP occupancy could allow us to understand the relationship between target engagement and degradation more broadly across our panel.[23,24] As inhibition of H3K18Ac by **8**−**19** provides a combined measure of cellular accumulation and EP300/CREBBP binding, we hypothesized it could be used to determine if HAT engagement is predictive of degradation. In contrast, observing efficient inhibition of H3K18Ac without degradation may reflect a molecule's inability to form a productive protein-degrader-E3 ternary complex. Assayed at two concentrations, **10** and **11** were the most potent VHL-based inhibitors, while several molecules (**9**, **12**−**14**) had little impact on acetylation (Figure S6). CRBN-based compounds were overall more active as HAT inhibitors, in line with the cyclic imide warhead being more cell permeable.[25] However, HAT engagement did not strictly correlate with degradation. This is most evident in the observation that **16** and **18**—the most potent inhibitors of H3K18Ac in our panel (Figure S6)—did not affect levels of EP300 or CREBBP (Figure 2b).

Previous studies have found one mechanism by which nonselective inhibitors can achieve specific degradation is by driving selective ternary complex formation with a subset of targets.[12] This observation, together with the finding that target engagement appears to be necessary but not sufficient for EP300-selective degradation, led us to further investigate the ability of our molecules to nucleate an EP300-VHL-degrader ternary complex. Here again we focused on compound **10**, "MC-1" (Figure 3a). To monitor EP300-VHL interactions in real time in living cells, we employed a luciferase complementation assay based on split Nanoluc.[26] Briefly, plasmid constructs were prepared in which the EP300 catalytic core consisting of the HAT and bromodomain (amino acids 1048−1665) was fused at the C-terminus to an inactive Nanoluc protein (LgBIT), and full length VHL was fused to a complementary fragment (SmBIT; Figure 3b). Coexpression of these proteins does not reconstitute Nanoluc activity due to their low intrinsic affinity but can be stimulated by compounds capable of nucleating formation of a stable ternary complex. Following optimized transfection of HEK-293T cells with

https://doi.org/10.1021/jacsau.4c00442
JACS Au 2024, 4, 3094−3103

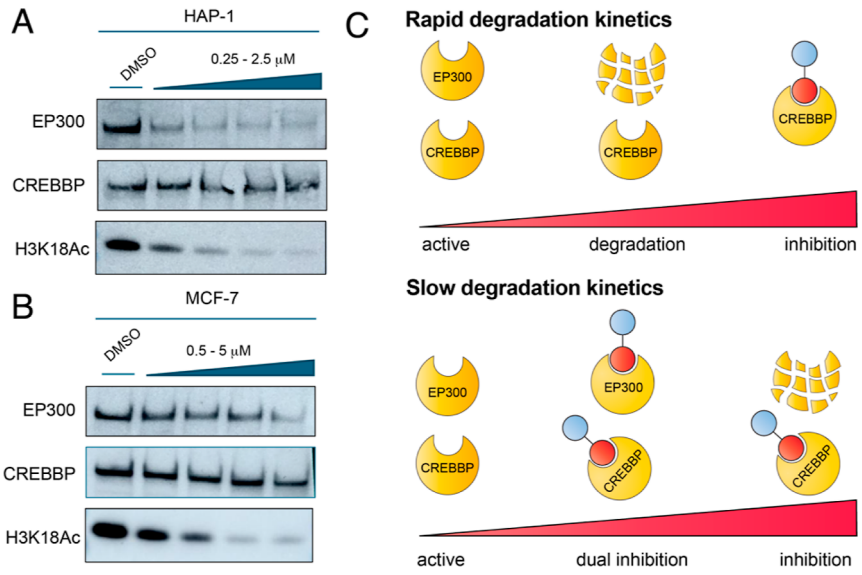

Figure 5. (A) Comparative effects of MC-1 on EP300 degradation and histone acetylation in HAP-1 cells. MC-1 was dosed at 0.25, 0.5, 1, and 2.5 μM for 6 h. (B) Comparative effects of MC-1 on EP300 degradation and histone acetylation in MCF-7 cells. MC-1 was dosed at 0.5, 1, 2.5, and 5 μM for 6 h (higher concentrations than in HAP-1 cells to observe clear degradation and inhibition). (C) Concentration and cell-dependent effects of HAT-based degraders. In cells where EP300 displays rapid degradation kinetics (HAP-1), MC-1 can significantly deplete EP300 while leaving CREBBP HAT activity intact. In cells where EP300 displays slower degradation kinetics (MCF-7), MC-1 can co-occupy and inhibit EP300 and CREBBP prior to EP300 degradation.

plasmids expressing C-terminal EP300-LgBIT and N-terminal SmBIT-VHL (Figure S7), the Nanoluc substrate furimazine was added and allowed to equilibrate.

Addition of MC-1 induced a rapid increase in Nanoluc activity, consistent with ternary complex formation (Figure 3c). Treatment of cells with CPI-1612 or vehicle [dimethyl sulfoxide (DMSO)] did not cause a similar response. Performing an identical assay but replacing the EP300 with the CREBBP catalytic core also yielded an induction of Nanoluc signal consistent with nucleation of a HAT-VHL interaction (Figure S8). This indicates that at least in the context of ectopic overexpression, MC-1 can form ternary complexes with both EP300/VHL and CREBBP/VHL. Further experimentation found EP300 degradation by MC-1 to be dose-dependent (Figure 3d), time-dependent (Figure 3e), and sensitive to "squelching" by free VHL ligand (Figure 3f) as well as CPI-1612 itself (Figure 3g). These data support the notion that MC-1 functions via ternary complex formation, but do not provide any evidence that selective ternary complex formation governs preferential degradation of EP300 versus CREBBP.

To investigate the broader impact of MC-1 on protein levels within cells, we conducted TMT-based proteomic profiling. These experiments compared HAP-1 cells treated with MC-1 (1 μM, 6 h) to control cells treated with vehicle DMSO. We also assessed dCBP-1 (250 nM, 6 h), using it as a validated probe known to degrade both EP300 and CREBBP. To maximize coverage, samples were extracted and subject to offline fractionation prior to tandem-mass tag labeling and pooled analysis. This strategy enabled the identification of >8400 quantified proteins (Table S2). We defined a significant change in protein level as having a p-value less than 0.05 and a log 2 fold change ratio of −0.6 (MC1-treated/DMSO-treated) and limited our reporter ion quantitation to unique peptides due to the high sequence identity of EP300 and CREBBP. The number of PSMs assigned to CREBBP (19) and EP300 (9) are high enough to infer accurate quantitation in specifically comparing these two paralogues. Remarkably, this analysis revealed EP300 as the only HAT degraded upon MC-1 treatment (Figure 4a). Applying similar criteria to dCBP-1 validated the ability of this probe to potently degrade both EP300 and CREBBP (Figure 4b). Treatment of cells with MC-1 for 6 h also changed the abundance of additional proteins unrelated to histone acetylation, perhaps unsurprising given the centrality of EP300 to transcriptional homeostasis. The only one of these proteins exhibiting a log2 fold decrease >0.6 was the alternative splicing regulator NOVA2. Dual degrader dCBP-1 caused a larger proteomic perturbation than MC-1. Interestingly, dCBP-1 also regulated NOVA2. Given the disparate structures of MC-1 and dCBP-1, we hypothesize that NOVA2 likely represents a protein highly sensitive to EP300 degradation in HAP-1 cells as opposed to an off-target. To further understand the downstream proteins affected by EP300 degradation we also analyzed MC-1 and dCBP-1 treated cells using data-independent acquisition (DIA) proteomics, which often shows improved capture of changes in low-abundance proteins (Table S3, Figure S9). This data set again showed potent degradation of EP300 over CREBBP across 6411 robustly quantified proteins and highlighted DLX5 and PDGFRA as additional proteins sensitive to EP300/CREBBP degradation (Figure S9). These findings define the proteome-wide selectivity of a paralogue-specific EP300 degrader.

Next, MC-1's activity was tested in a broader context by examining its activity in the NCI60 cell line screen (Figure 4c). This analysis used a recently redesigned, miniaturized version of the screen which employs a 384-well plate format, ATP-based viability readout, and 72 h treatment regimen.[27] To benchmark MC-1's activity we also tested the previously reported dual EP300/CREBBP degrader dCBP-1 as well as the EP300-specific degrader JQAD-1. All three compounds were tested across five concentrations in order to calculate half-

https://doi.org/10.1021/jacsau.4c00442
JACS Au 2024, 4, 3094−3103

maximal growth inhibition (GI_{50}). All three molecules were active against HL-60, CCRF-CEM, and MOLT-4 cells. This is consistent with the known dependence of hemopoietic malignancies on acetylation-dependent transcription.[1] In terms of broader trends, MC-1 appeared to potently inhibit a unique subset of cell lines relative to JQAD-1 and dCBP-1 which were narrowly and broadly active, respectively. Quantitative dose−response profiling confirmed that MC-1 inhibited cell proliferation in MCF-7 cells, while HAP-1 cells were relatively unaffected (Figure S10). Understanding that growth inhibition could be the result of either degradation or catalytic inhibition, we examined the dose-dependent effects of MC-1 on EP300, CREBBP, and H3K18Ac in these models. In HAP-1 cells, EP300 degradation occurs at low concentrations and appears to slightly precede complete loss of H3K18Ac caused by the dual inhibition of the EP300 and CREBBP HAT domains (Figure 5a). This is consistent with prior work characterizing acute EP300 degradation by JQAD-1.[17] Similarly, when cells are allowed to rebound from treatment with concentrations of the small molecule that inhibit H3K18Ac, acetylation is recovered prior to EP300 (Figure S11). MCF-7 cells display the opposite profile. Here, degradation occurs only to a limited extent at higher concentrations and appears to trail HAT inhibition (Figure 5b). We hypothesize this may reflect different degradation kinetics in the two cell lines (Figure 5c), potentially driven by increased drug efflux, reduced E3 ligase levels, or rapid rates of EP300 resynthesis. Previous studies have mentioned the potential for specific degraders to cause concentration-dependent catalytic inhibition,[12,28] although this has rarely been explored across multiple cell lines. Our results confirm the activity of paralogue-specific EP300 degraders and provide an approach for assessing dual inhibition versus paralogue-specific degradation.

Here we report selective chemical degradation of the histone acetyltransferase EP300. Our studies complement significant previous efforts in the field but differentiate themselves by demonstrating for the first time that a potent HAT ligand in combination with VHL recruitment affords preferential degradation of EP300 over its closely related paralogue, CREBBP. Mechanistic studies indicate that selective degradation of EP300 by a bifunctional ligand cannot be predicted by measurement of target engagement (as assessed by inhibition of H3K18Ac) or ability to form a HAT-VHL-degrader ternary complex (as assessed by NanoBiT complementation assay). Instead, our results are most consistent with EP300's (i) slightly increased binding affinity for CPI-1612, (ii) higher confidence predicted interactions with VHL, and (iii) possession of two nonconserved lysine residues relative to CREBBP. Previous studies of p38 MAPK degraders have found ternary complex formation is necessary but not sufficient to explain degrader selectivity.[29] Defining the downstream factors that govern selective EP300 degradation will be an important step for extending and improving this approach.

As currently constituted, we envision MC-1 will find utility studies aimed at differentiating the noncatalytic roles of EP300 and CREBBP, particularly in cell lines which are not greatly affected by loss of EP300/CREBBP HAT activity. In addition, it is known that ligands targeting the HAT domain of EP300/CREBBP are sensitive to cellular acetyl-CoA levels.[10,30] While the ability of MC-1 to inhibit acetylation in MCF-7 implies acetyl-CoA is not solely responsible for the limited degradation observed in this cell line, these studies suggest the possibility of leveraging metabolite-competitive degradation to study cellular acetyl-CoA, an application that could provide valuable insights into metabolic signaling.[31]

We also note limitations of our study and future directions of inquiry. First, our analysis of growth inhibition across the NCI-60 does not differentiate death caused by paralogue-specific degradation from dual catalytic inhibition. Indeed, at high concentrations (e.g., 100 μM, the highest concentration used in the screen) dual catalytic inhibition could be a dominant driver of toxicity even in cell lines that are not susceptible to deletion of EP300 alone. Differentiating degradation-dependent versus catalysis-dependent effects will require more closely mimicking CRISPR screening conditions by analyzing growth inhibition upon long-term treatment at low (subinhibitory) concentrations of MC-1 and comparison to inactive degrader compounds. A second limitation is that MC-1 does not completely abolish cellular EP300. It caused a maximal degradation of ∼85% in our HAP-1 model and considerably less in MCF-7 cells. This, along with the observation that JQAD-1 was inactive in HAP-1 cells (Figure S2), raises the question as to the degree to which cell line specificity may be a broader attribute of paralogue-specific EP300 degraders. For example, JQAD-1's mechanism was recently validated in a study showing that CRBN KO confers resistance in several models,[32] but this was observed in only 9/19 cell lines tested. MC-1's ability to inhibit H3K18Ac in MCF-7 would argue against differential occupancy being the sole determinant of this variability. Other criteria that may influence degradation include cellular accumulation, E3 ligase activity, bromodomain occupancy (Figure S12), and the ability of EP300 partner proteins[33] to influence accessibility and correct orientation of the ubiquitinylation machinery. During preparation of this manuscript a CPI-1612-derived CRBN-based dual EP300/CREBBP degrader was reported.[21] This ever-expanding toolbox of HAT domain-targeting degraders, in combination with chemical and genetic screens, should be helpful in identifying factors underlying cell-type specific degradation.

Our studies also emphasize the emerging spectrum of options for therapeutic EP300/CREBBP inhibition. In addition to the well-characterized HAT[10] and BRD[34−36] ligands, there are now multiple potent dual degraders based on BRD ligands.[13−16,37] JQAD-1 and MC-1 add to this collection by affording paralogue-specific degradation and—in the case of MC-1, and possibly JQAD-1 as well—dual HAT inhibition at high concentrations. In this latter scenario, MC-1 may be deployed as an augmented HAT inhibitor with an additional capability to degrade EP300. Interestingly, a recent study reported that dual EP300/CREBBP degraders do not cause weight loss in mice.[38] This implies either that dual loss of EP300/CREBBP catalytic activity is more well-tolerated than expected, or that the unique pharmacology of bifunctional molecules may spare EP300/CREBBP in settings where it is essential. Related to this, VHL-linked degraders have shown the capacity to mitigate thrombocytopenia caused by their parent inhibitor compounds in platelet models.[39] Whether MC-1 or improved derivatives will show similarly altered safety or efficacy is currently unknown. These studies are underway and will be reported in due course.

https://doi.org/10.1021/jacsau.4c00442
JACS Au 2024, 4, 3094−3103

■ ASSOCIATED CONTENT

Data Availability Statement

The mass spectrometry proteomics data have been deposited to the MassIVE repository with the dataset identifier MSV000094896.

Supporting Information

The Supporting Information is available free of charge at https://pubs.acs.org/doi/10.1021/jacsau.4c00442.

Supplementary figures, methods and materials for all experiments including synthetic details, and complete Western blots (PDF)

TMTpro channel assignments (XLSX)

Data independent acquisition (DIA) LC-MS/MS proteomics analysis of proteomic changes induced by MC-1 and dCBP-1(XLSX)

■ AUTHOR INFORMATION

Corresponding Author

Jordan L. Meier − *Chemical Biology Laboratory, National Cancer Institute, Frederick, Maryland 21702, United States;* orcid.org/0000-0002-0537-7101; Email: jordan.meier@nih.gov

Authors

Xuemin Chen − *Chemical Biology Laboratory, National Cancer Institute, Frederick, Maryland 21702, United States*

McKenna C. Crawford − *Chemical Biology Laboratory, National Cancer Institute, Frederick, Maryland 21702, United States;* orcid.org/0000-0002-3274-1255

Ying Xiong − *Chemical Biology Laboratory, National Cancer Institute, Frederick, Maryland 21702, United States*

Anver Basha Shaik − *Chemistry and Synthesis Center, National Heart Lung and Blood Institute, Rockville, Maryland 20850, United States*

Kiall F. Suazo − *Chemical Biology Laboratory, National Cancer Institute, Frederick, Maryland 21702, United States; Protein Characterization Laboratory, Frederick National Laboratory for Cancer Research, Leidos Biomedical Research, Frederick, Maryland 21701, United States*

Ludwig G. Bauer − *Centre for Medicines Discovery, Nuffield Department of Medicine, University of Oxford, Oxford OX3 7FZ, U.K.;* orcid.org/0000-0002-2235-3945

Manini S. Penikalapati − *Chemical Biology Laboratory, National Cancer Institute, Frederick, Maryland 21702, United States*

Joycelyn H. Williams − *Chemical Biology Laboratory, National Cancer Institute, Frederick, Maryland 21702, United States*

Kilian V. M. Huber − *Centre for Medicines Discovery, Nuffield Department of Medicine, University of Oxford, Oxford OX3 7FZ, U.K.;* orcid.org/0000-0002-1103-5300

Thorkell Andressen − *Protein Characterization Laboratory, Frederick National Laboratory for Cancer Research, Leidos Biomedical Research, Frederick, Maryland 21701, United States*

Rolf E. Swenson − *Chemistry and Synthesis Center, National Heart Lung and Blood Institute, Rockville, Maryland 20850, United States*

Complete contact information is available at: https://pubs.acs.org/10.1021/jacsau.4c00442

Author Contributions

⊥These authors contributed equally. CRediT: **Xuemin Chen** conceptualization, data curation, formal analysis, funding acquisition, investigation, methodology, project administration, resources, software, supervision, validation, visualization, writing-original draft, writing-review & editing; **McKenna C. Crawford** conceptualization, data curation, formal analysis, funding acquisition, investigation, methodology, project administration, resources, software, supervision, validation, visualization, writing-original draft, writing-review & editing; **Ying Xiong** conceptualization, data curation, formal analysis, funding acquisition, investigation, methodology, project administration, resources, software, supervision, validation, visualization, writing-original draft, writing-review & editing; **Anver Basha Shaik** conceptualization, data curation, formal analysis, investigation, methodology, project administration, resources, software, supervision, validation, visualization, writing-original draft, writing-review & editing; **Kiall Suazo** conceptualization, data curation, formal analysis, investigation, methodology, writing-review & editing; **Ludwig G. Bauer** conceptualization, data curation, formal analysis, investigation, methodology; **Manini S. Penikalapati** investigation, methodology, validation; **Joycelyn H Williams** investigation, methodology, validation; **Kilian V. M. Huber** conceptualization, data curation, formal analysis, investigation, methodology, funding acquisition, writing-review & editing; **Thorkell Andresson** investigation, methodology, project administration; **Rolf E. Swenson** conceptualization, formal analysis, funding acquisition, project administration; **Jordan L. Meier** conceptualization, funding acquisition, project administration, resources, supervision, writing-original draft, writing-review & editing.

Notes

The authors declare no competing financial interest.

■ ACKNOWLEDGMENTS

The authors thank Dr. Francis O'Reilly (NCI), Beverly Mock (NCI) and Snehal Gaikwad (NCI) for helpful discussions and experimental materials. We are grateful to Prof. Jun Qi (DFCI) for supplying JQAD-1. This work was supported by the Intramural Research Programs of the National Cancer Institute, Center for Cancer Research ZIA BC011488. This work utilized the computational resources of the NIH HPC Biowulf cluster (http://hpc.nih.gov). This project received funding from the Innovative Medicines Initiative 2 Joint Undertaking (JU) under grant agreement no 875510. The JU receives support from the European Union's Horizon 2020 research and innovation program, the European Federation of Pharmaceutical Industries and Associations (EFPIA), the Ontario Institute for Cancer Research, the Royal Institution for the Advancement of Learning McGill University, the KTH Royal Institute of Technology (Kungliga Tekniska Hoegskolan), and Diamond Light Source Limited.

■ REFERENCES

(1) Dancy, B. M.; Cole, P. A. Protein lysine acetylation by p300/CBP. *Chem. Rev.* **2015**, *115* (6), 2419−2452.

(2) Farria, A.; Li, W.; Dent, S. Y. KATs in cancer: functions and therapies. *Oncogene* **2015**, *34* (38), 4901−4913.

(3) Wang, L.; Gural, A.; Sun, X. J.; Zhao, X.; Perna, F.; Huang, G.; Hatlen, M. A.; Vu, L.; Liu, F.; Xu, H.; et al. The leukemogenicity of AML1-ETO is dependent on site-specific lysine acetylation. *Science* **2011**, *333* (6043), 765−769.

(4) Liu, Y.; Wang, L.; Predina, J.; Han, R.; Beier, U. H.; Wang, L. C.; Kapoor, V.; Bhatti, T. R.; Akimova, T.; Singhal, S.; et al. Inhibition of p300 impairs Foxp3(+) T regulatory cell function and promotes antitumor immunity. *Nat. Med.* **2013**, *19* (9), 1173−1177.
(5) Ogiwara, H.; Sasaki, M.; Mitachi, T.; Oike, T.; Higuchi, S.; Tominaga, Y.; Kohno, T. Targeting p300 Addiction in CBP-Deficient Cancers Causes Synthetic Lethality by Apoptotic Cell Death due to Abrogation of MYC Expression. *Cancer Discov.* **2016**, *6* (4), 430−445.
(6) Rebel, V. I.; Kung, A. L.; Tanner, E. A.; Yang, H.; Bronson, R. T.; Livingston, D. M. Distinct roles for CREB-binding protein and p300 in hematopoietic stem cell self-renewal. *Proc. Natl. Acad. Sci. U.S.A.* **2002**, *99* (23), 14789−14794.
(7) Lasko, L. M.; Jakob, C. G.; Edalji, R. P.; Qiu, W.; Montgomery, D.; Digiammarino, E. L.; Hansen, T. M.; Risi, R. M.; Frey, R.; Manaves, V.; et al. Discovery of a selective catalytic p300/CBP inhibitor that targets lineage-specific tumours. *Nature* **2017**, *550* (7674), 128−132.
(8) Whedon, S. D.; Cole, P. A. KATs off: Biomedical insights from lysine acetyltransferase inhibitors. *Curr. Opin. Chem. Biol.* **2023**, *72*, 102255.
(9) Wilson, J. E.; Patel, G.; Patel, C.; Brucelle, F.; Huhn, A.; Gardberg, A. S.; Poy, F.; Cantone, N.; Bommi-Reddy, A.; Sims, R. J., 3rd; et al. Discovery of CPI-1612: A Potent, Selective, and Orally Bioavailable EP300/CBP Histone Acetyltransferase Inhibitor. *ACS Med. Chem. Lett.* **2020**, *11* (6), 1324−1329.
(10) Crawford, M. C.; Tripu, D. R.; Barritt, S. A.; Jing, Y.; Gallimore, D.; Kales, S. C.; Bhanu, N. V.; Xiong, Y.; Fang, Y.; Butler, K. A. T.; et al. Comparative Analysis of Drug-like EP300/CREBBP Acetyltransferase Inhibitors. *ACS Chem. Biol.* **2023**, *18* (10), 2249−2258.
(11) Schapira, M.; Calabrese, M. F.; Bullock, A. N.; Crews, C. M. Targeted protein degradation: expanding the toolbox. *Nat. Rev. Drug Discov.* **2019**, *18* (12), 949−963.
(12) Brand, M.; Jiang, B.; Bauer, S.; Donovan, K. A.; Liang, Y.; Wang, E. S.; Nowak, R. P.; Yuan, J. C.; Zhang, T.; Kwiatkowski, N.; et al. Homolog-Selective Degradation as a Strategy to Probe the Function of CDK6 in AML. *Cell Chem. Biol.* **2019**, *26* (2), 300−306.e9. e309
(13) Vannam, R.; Sayilgan, J.; Ojeda, S.; Karakyriakou, B.; Hu, E.; Kreuzer, J.; Morris, R.; Herrera Lopez, X. I.; Rai, S.; Haas, W.; et al. Targeted degradation of the enhancer lysine acetyltransferases CBP and p300. *Cell Chem. Biol.* **2021**, *28* (4), 503−514.e12. e512
(14) Thomas, J. E., 2nd; Wang, M.; Jiang, W.; Wang, M.; Wang, L.; Wen, B.; Sun, D.; Wang, S. Discovery of Exceptionally Potent, Selective, and Efficacious PROTAC Degraders of CBP and p300 Proteins. *J. Med. Chem.* **2023**, *66* (12), 8178−8199.
(15) Chen, Z.; Wang, M.; Wu, D.; Zhao, L.; Metwally, H.; Jiang, W.; Wang, Y.; Bai, L.; McEachern, D.; Luo, J.; et al. Discovery of CBPD-409 as a Highly Potent, Selective, and Orally Efficacious CBP/p300 PROTAC Degrader for the Treatment of Advanced Prostate Cancer. *J. Med. Chem.* **2024**, *67* (7), 5351−5372.
(16) Chen, Z.; Wang, M.; Wu, D.; Bai, L.; Xu, T.; Metwally, H.; Wang, Y.; McEachern, D.; Zhao, L.; Li, R.; et al. Discovery of CBPD-268 as an Exceptionally Potent and Orally Efficacious CBP/p300 PROTAC Degrader Capable of Achieving Tumor Regression. *J. Med. Chem.* **2024**, *67* (7), 5275−5304.
(17) Durbin, A. D.; Wang, T.; Wimalasena, V. K.; Zimmerman, M. W.; Li, D.; Dharia, N. V.; Mariani, L.; Shendy, N. A. M.; Nance, S.; Patel, A. G.; et al. EP300 Selectively Controls the Enhancer Landscape of MYCN-Amplified Neuroblastoma. *Cancer Discov.* **2022**, *12* (3), 730−751.
(18) Jumper, J.; Evans, R.; Pritzel, A.; Green, T.; Figurnov, M.; Ronneberger, O.; Tunyasuvunakool, K.; Bates, R.; Zidek, A.; Potapenko, A.; et al. Highly accurate protein structure prediction with AlphaFold. *Nature* **2021**, *596* (7873), 583−589.
(19) Mirdita, M.; Schutze, K.; Moriwaki, Y.; Heo, L.; Ovchinnikov, S.; Steinegger, M. ColabFold: making protein folding accessible to all. *Nat. Methods* **2022**, *19* (6), 679−682.
(20) Pereira, G. P.; Gouzien, C.; Souza, P. C. T.; Martin, J. AlphaFold-Multimer struggles in predicting PROTAC-mediated protein-protein interfaces. *bioRxiv* **2024**, bioRxiv2024.03.19.585735.
(21) Cheng-Sanchez, I.; Gossele, K. A.; Palaferri, L.; Kirillova, M. S.; Nevado, C. Discovery and Characterization of Active CBP/EP300 Degraders Targeting the HAT Domain. *ACS Med. Chem. Lett.* **2024**, *15* (3), 355−361.
(22) Hanzl, A.; Barone, E.; Bauer, S.; Yue, H.; Nowak, R. P.; Hahn, E.; Pankevich, E. V.; Koren, A.; Kubicek, S.; Fischer, E. S.; Winter, G. E. E3-Specific Degrader Discovery by Dynamic Tracing of Substrate Receptor Abundance. *J. Am. Chem. Soc.* **2023**, *145* (2), 1176−1184.
(23) Jin, Q.; Yu, L. R.; Wang, L.; Zhang, Z.; Kasper, L. H.; Lee, J. E.; Wang, C.; Brindle, P. K.; Dent, S. Y.; Ge, K. Distinct roles of GCN5/PCAF-mediated H3K9ac and CBP/p300-mediated H3K18/27ac in nuclear receptor transactivation. *EMBO J.* **2011**, *30* (2), 249−262.
(24) Feller, C.; Forne, I.; Imhof, A.; Becker, P. B. Global and specific responses of the histone acetylome to systematic perturbation. *Mol. Cell* **2015**, *57* (3), 559−571.
(25) Foley, C. A.; Potjewyd, F.; Lamb, K. N.; James, L. I.; Frye, S. V. Assessing the Cell Permeability of Bivalent Chemical Degraders Using the Chloroalkane Penetration Assay. *ACS Chem. Biol.* **2020**, *15* (1), 290−295.
(26) Dixon, A. S.; Schwinn, M. K.; Hall, M. P.; Zimmerman, K.; Otto, P.; Lubben, T. H.; Butler, B. L.; Binkowski, B. F.; Machleidt, T.; Kirkland, T. A.; et al. NanoLuc Complementation Reporter Optimized for Accurate Measurement of Protein Interactions in Cells. *ACS Chem. Biol.* **2016**, *11* (2), 400−408.
(27) Morris, J.; Kunkel, M. W.; White, S. L.; Wishka, D. G.; Lopez, O. D.; Bowles, L.; Sellers Brady, P.; Ramsey, P.; Grams, J.; Rohrer, T.; et al. Targeted Investigational Oncology Agents in the NCI-60: A Phenotypic Systems-based Resource. *Mol. Cancer Ther.* **2023**, *22* (11), 1270−1279.
(28) Potjewyd, F.; Turner, A. W.; Beri, J.; Rectenwald, J. M.; Norris-Drouin, J. L.; Cholensky, S. H.; Margolis, D. M.; Pearce, K. H.; Herring, L. E.; James, L. I. Degradation of Polycomb Repressive Complex 2 with an EED-Targeted Bivalent Chemical Degrader. *Cell Chem. Biol.* **2020**, *27* (1), 47−56.e15. e15
(29) Smith, B. E.; Wang, S. L.; Jaime-Figueroa, S.; Harbin, A.; Wang, J.; Hamman, B. D.; Crews, C. M. Differential PROTAC substrate specificity dictated by orientation of recruited E3 ligase. *Nat. Commun.* **2019**, *10* (1), 131.
(30) Bishop, T. R.; Subramanian, C.; Bilotta, E. M.; Garnar-Wortzel, L.; Ramos, A. R.; Zhang, Y.; Asiaban, J. N.; Ott, C. J.; Rock, C. O.; Erb, M. A. Acetyl-CoA biosynthesis drives resistance to histone acetyltransferase inhibition. *Nat. Chem. Biol.* **2023**, *19* (10), 1215−1222.
(31) Trefely, S.; Lovell, C. D.; Snyder, N. W.; Wellen, K. E. Compartmentalised acyl-CoA metabolism and roles in chromatin regulation. *Mol. Metab.* **2020**, *38*, 100941.
(32) Lee, H. M.; Wright, W. C.; Pan, M.; Low, J.; Currier, D.; Fang, J.; Singh, S.; Nance, S.; Delahunty, I.; Kim, Y.; et al. A CRISPR-drug perturbational map for identifying compounds to combine with commonly used chemotherapeutics. *Nat. Commun.* **2023**, *14* (1), 7332.
(33) Bedford, D. C.; Brindle, P. K. Is histone acetylation the most important physiological function for CBP and p300? *Aging* **2012**, *4* (4), 247−255.
(34) Crawford, T. D.; Romero, F. A.; Lai, K. W.; Tsui, V.; Taylor, A. M.; de Leon Boenig, G.; Noland, C. L.; Murray, J.; Ly, J.; Choo, E. F.; et al. Discovery of a Potent and Selective in Vivo Probe (GNE-272) for the Bromodomains of CBP/EP300. *J. Med. Chem.* **2016**, *59* (23), 10549−10563.
(35) Hay, D. A.; Fedorov, O.; Martin, S.; Singleton, D. C.; Tallant, C.; Wells, C.; Picaud, S.; Philpott, M.; Monteiro, O. P.; Rogers, C. M.; et al. Discovery and optimization of small-molecule ligands for the CBP/p300 bromodomains. *J. Am. Chem. Soc.* **2014**, *136* (26), 9308−9319.
(36) Welti, J.; Sharp, A.; Brooks, N.; Yuan, W.; McNair, C.; Chand, S. N.; Pal, A.; Figueiredo, I.; Riisnaes, R.; Gurel, B.; et al. Targeting

https://doi.org/10.1021/jacsau.4c00442
JACS Au 2024, 4, 3094−3103

the p300/CBP Axis in Lethal Prostate Cancer. *Cancer Discov.* **2021**, *11* (5), 1118−1137.
(37) Hu, J.; Xu, H.; Wu, T.; Zhang, C.; Shen, H.; Dong, R.; Hu, Q.; Xiang, Q.; Chai, S.; Luo, G.; et al. Discovery of Highly Potent and Efficient CBP/p300 Degraders with Strong In Vivo Antitumor Activity. *J. Med. Chem.* **2024**, *67*, 6952−6986.
(38) Luo, J.; Chen, Z.; Qiao, Y.; Ching-Yi Tien, J.; Young, E.; Mannan, R.; Mahapatra, S.; He, T.; Eyunni, S.; Zhang, Y.; et al. p300/CBP degradation is required to disable the active AR enhanceosome in prostate cancer. *bioRxiv* **2024**, bioRxiv2024.03.29.587346.
(39) Khan, S.; Zhang, X.; Lv, D.; Zhang, Q.; He, Y.; Zhang, P.; Liu, X.; Thummuri, D.; Yuan, Y.; Wiegand, J. S.; et al. A selective BCL-X(L) PROTAC degrader achieves safe and potent antitumor activity. *Nat. Med.* **2019**, *25* (12), 1938−1947.

https://doi.org/10.1021/jacsau.4c00442
JACS Au 2024, 4, 3094−3103